Visualization of Liquid Fuel Behavior in a Spark Ignition Engine during Starting and Warm-up

Younggy Shin*

(*Received February 17, 1997*)

The liquid fuel behavior in the intake port and the cylinder during starting and warm-up was visualized through visualization windows using a high speed CCD camera. The videos were taken with the engine firing under cold conditions in the simulated start-up process, at 1,000 and 1,200 RPM and intake manifold pressure of 0.5 bar. The variables examined were the injector geometry and injector type (normal and air-assisted). The visualization results show several features of the liquid fuel behavior: 1) backward strip-atomization of the fuel film along the periphery of the intake valves by the valve overlap backflow; 2) forward strip-atomization of the fuel film on the surfaces of the intake system into droplet streams by the intake air flow; 3) film flow which forms significant liquid puddles at the valve surface and at the vicinity of the intake valve; and 4) squeezing of the liquid film at the valve lip and seat into large droplets in the valve closing process. Some of the liquid fuel survives combustion into the next cycle. The time evolution of the in-cylinder liquid film is influenced by the injection geometry and port surface temperature. Photographs showing the liquid fuel features and an explanation of the observed phenomena are given in the paper.

Key Words: Liquid Fuel, Starting, Warm-Up, Visualization, CCD Camera, High Speed Photography, Fuel Film, Hydrocarbon Emissions, Mixture Preparation, Fuel Injector, Spark Ignition Engine

Nomenclature

A/F : Air-to-fuel ratio
CA : Crank angle
g : Gravity
IVC : Intake valve closing
IVO : Intake valve opening
MBT : Maximum brake torque
TC : Top center
u : Velocity
V : Velocity

Greek symbols

δ : Film thickness
λ : Excess air ratio
μ : Dynamic viscosity
ρ : Density
σ : Surface tension

* Sloan Automotive Lab., Massachusetts Institute of Technology, cambridge MA, U.S.A.

1. Introduction

A plausible mechanism for hydrocarbon (HC) emissions is the entry of liquid fuel into the engine cylinder. This is especially critical in the engine starting process due to poor fuel evaporation in the cold engine. To achieve smooth starting, fuel enrichment is used so that there is sufficient vaporized fuel to form a combustible mixture in the engine cylinder. A substantial amount of the injected fuel, especially the less volatile components, does not vaporize (Cheng et al., 1993; Fox et al., 1992) and enters into the cylinder as liquid. This fuel may be stored somewhere in the cylinder (such as in the deposit, oil layer or crevices in the combustion chamber) and comes out into the bulk gas in the expansion and exhaust processes. The incomplete oxidation of this fuel would contribute to the exhaust HC emissions.

In spite of the significant contribution of the liquid fuel effect to the HC emissions during engine starting and warm-up, liquid fuel behavior in the engine cylinder has been poorly understood. This is because of the difficulty associated with observing the liquid fuel in the cylinder of a practical engine due to the lack of optical access; and that the phenomenon cannot be easily reproduced in a bench scale flow rig because processes such as the back flow of the hot burned gas from the cylinder to the intake port in a firing engine could not be reproduced easily.

The purpose of this paper is to show the important features of the liquid fuel entry into the engine cylinder and the behavior of the liquid fuel deposited on the combustion chamber wall through the engine cycle. The liquid fuel is visualized using a high-speed CCD camera in the firing engines which have optical access to their inside.

2. Experimental Apparatus

2.1 Test engine for in-cylinder visualization

To visualize the liquid fuel behavior within the cylinder, it is desirable to use the transparent engine with the following features:

1) the windows for visualization in the engine should be easily taken apart for frequent cleaning since unvaporized liquid fuel tends to make the window dirty in a short period of time;

2) the windows should be wide enough to admit adequate lighting and to accommodate various camera view angles;

3) the windows should withstand the thermal loading of engine firing.

In order to satisfy the above requirements, the following experimental apparatus was used.

Figure 1 shows a schematic of the single-cylinder transparent visualization engine (Namazian et al., 1980) that was used in this study. The engine has the square cross-section cylinder assembly with two opposing glass walls which serve as windows for ease of optical access. The glass walls could easily be taken apart from the engine without disassembling other parts. The square piston is sealed by graphite seal bars that overlap at the corners and these bars are pressed against the cylinder walls by springs from behind. The graphite seals provide the dry means of sealing the combustion chamber so that the windows are not obscured by the lubrication oil. Details of the engine configuration are listed in Table 1.

Table 1 Geometrical data of square piston engine

Displacement Volume	785 cm^3
Stroke	114.3 mm
Side	82.6 mm
Connecting Rod Length	254 mm
Compression Ratio	6.07
Valve Timing	IVO 10°ATC
	IVC 25°ABC
	EVO 45°ABC
	EVC 10°ATC

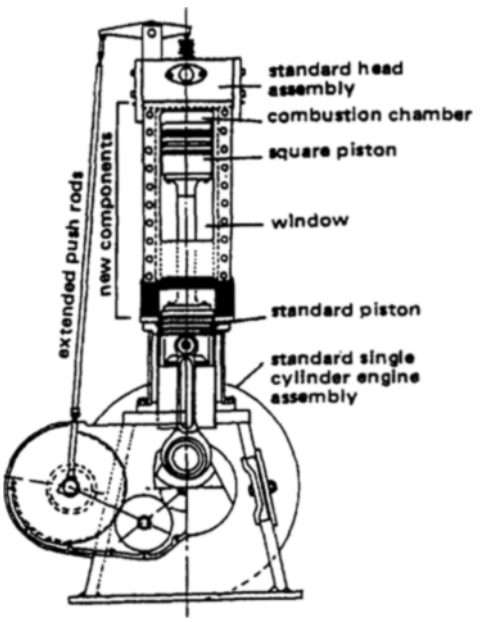

Fig. 1 Schematic of a square piston engine

The high speed CCD camera used in this study was a Kodak Ektapro system. The sensor consists of an 192×239 pixel NMOS array. The recording rates used for the current set of experiments were 500, 1,000 and 2,000 frames/sec. A 90 mm f/2.5 camera lens was used for imaging. The field of view was illuminated by a collimated 650W can-

Table 2 Volvo B5254 Engine specification

Displacement Volume	487.0 cm^3
Stroke	90.0 mm
Bore	83.0 mm
Connecting Rod Length	158.0 mm
Compression Ratio	10.1
Valve Timing	IVO 4°ATC
	IVC 56°ABC
	EVO 48°ABC
	EVC 12°ATC

descent light source which was carefully placed to avoid direct reflection of the light into the camera. The images were recorded in image files and transferred onto video tapes.

2.2 Test engine for intake port visualization

The intake port visualization was done on the single cylinder engine which was converted from a commercial five-cylinder engine (the Volvo B5254 Engine for the Volvo 850 vehicle). The engine was of modern design with DOHC, 4-valves per cylinder and a pent-roof fast-burn combustion chamber. A section of the head of the engine was sawed off and fit on a Ricardo Hydra single-cylinder engine block. The liner, piston and crank shaft were outfit to be the same as the commercial engine. The engine specification is listed in Table 2. Fuel was injected at the port with a Bosch EV1.1A injector which supplied a hollow-cone spray of 20° cone angle (Fig. 2). The fuel spray was split so that nominally half of the fuel went into each of the intake valves. The fuel was injected when the valves were closed. The Sauter Mean Diameter was ~130 mm. The fuel used in the experiment was indolene, which is a gasoline manufactured under tight specifications. It has a Reid Vapor Pressure of 0.6 bar. The 10, 50 and 90 % distillation points are at 53.3, 105 and 151.7℃.

To observe the fuel injection and induction process in the intake port, the intake runner had been replaced so that windows could be fit for illumination and observation (Fig. 2). The injector position and the section of the runner

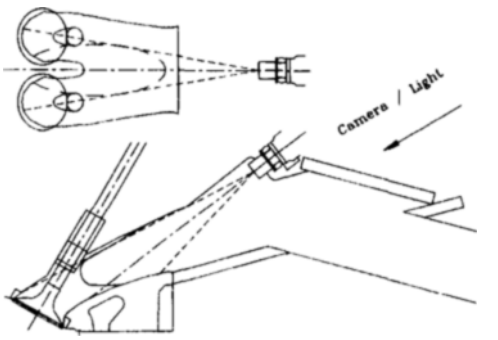

Fig. 2 Fuel injection geometry of a Volvo engine

between the windows and the head were unchanged. The modification should not substantially affect the engine behavior. This was confirmed by verifying that the modified engine performance was the same as the unmodified one.

The "windows" were actually built by replacing a section of the runner with the rhombic section which consisted of a metal base plate and three large glass walls. The intake port region could be seen clearly through the glass walls. The camera was placed behind the top glass wall (Fig. 2). The illumination was through the side wall. Collimated light from a 300 watt CW xenon arc lamp was used for illumination.

The images of the intake process were captured on video at 500 frames per second by a Kodak Ektapro high speed video camera. At the test condition (1200 rpm), the camera recorded at 14.4 crank-angle between frames. The intake event (IVO to IVC) was captured in ~17 frames and the injection event, in ~6 frames. The framing rate was fast enough to identify the important gross features in the mixing preparation process. There was no attempt, however, to identify the evaporation and transport behavior of individual droplets.

3. Engine Operating Conditions

3.1 In-cylinder visualization

In the simulated starting experiments, the engine was motored at 1,000 rpm and the throttle position was fixed at the intake manifold pressure of 0.5~0.6 bar. Then fuel injection (with the fixed pulse width) started. Since the engine had

no cooling system, the engine was only fired for approximately 2 minutes until the cylinder wall temperature reached 100 ℃. After each run, the engine was cooled down before the next run to keep the initial temperatures of the engine and intake system at 20 ℃. The air-to-fuel ratio was preset to become stoichiometry when the engine was under steady firing. The amount of fuel injected was calibrated by the measured values using a wide-range lambda meter and a laminar flow meter (for the air flow) taken at the end of the engine warm-up test at which there was complete vaporization of the liquid fuel. The injection timing corresponded to closed-valve-injection (injection started at 205 degrees after non-firing TC).

Two types of fuel injectors were used to compare the effects of intake port wetting area due to fuel injection geometry on in-cylinder liquid fuel behavior. Figure 3(a) shows the fuel injection geometry in the intake port equipped with a normal injector (Bosch EV1.1A). The Sauter Mean Diameter for this injector is about 130 μm. It is noted that the intake port geometry in this engine (which was constructed using the head of a CFR engine) is substantially different from that of modern engines. As seen in the figure, the injected fuel spray did not hit the back of the intake valve directly and, as a result, there was substantial fuel wetting over a wide area of the port. Figure 3(b) is a drawn-to-scale drawing showing the fuel injection geometry in the intake port equipped with an air-assisted injector provided by the Ford Motor company (Yang et al., 1993). It was designed to minimize wall wetting and to improve atomization by shattering the fuel drops with an air jet supplied by compressed air at about 0.68 bar gauge pressure. Although the SMD (Sauter Mean Diameter) of the fuel spray was reported to be about 40 μm (Yang et al., 1993), the improvement in atomization was believed to have much less impact in this port configuration since the distance between the injector tip and the impinging surface of the intake valve was rather short so that most of the fuel impinged on the back of the intake valve. Therefore, the main purpose of using the air-assisted injector in this test was to change the injection geometry and to minimize the wall wetting area.

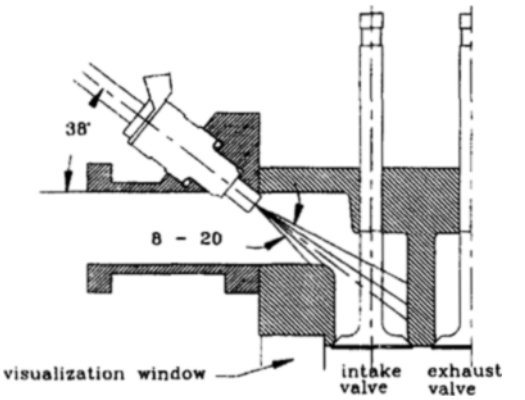

(a) A normal fuel injector

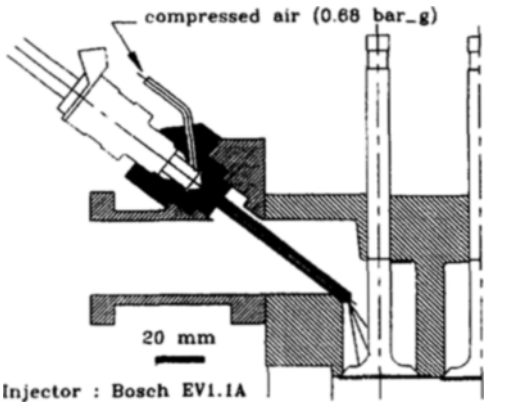

(b) An air-assisted fuel injector

Fig. 3 Fuel injection geometry in the square-section visualization engine

3.2 Intake port visualization

The intake process was observed at 1200 rpm and at 0.5 bar intake pressure. The spark timing was fixed at 30° BTC which was the MBT timing. The coolant temperature at the head was kept at 25 °C. A stoichiometric amount of fuel was injected. Injection was from 336 °CA to −249 °CA before the intake valve opening during which the intake valves were closed. The amount of fuel injected was ~20 mg per pulse. The engine was firing at the steady state condition. The test condition is representative of that of the engine at the first cycle of the FTP emissions test during which the engine is running steadily but the wall temper-

atures are still quite low.

4. Visualization Results; Description of Liquid Fuel Behavior over One Cycle

The visualization results obtained in a typical engine cycle during the warm-up process is discussed in this section. The sequence of events that governs the liquid fuel behavior is illustrated in Fig. 4.

When the fuel is injected into the intake port, it wets the port walls and intake valves under the footprint of the fuel spray. In the case of closed valve injection timing, the injected liquid fuel flows down toward the lower periphery of the intake valve due to the gravity force acting on the fuel film. The gravity effect is observed from the port visualization results shown in Fig. 5. The comparison of Fig. 5(b) and 5(d) clearly shows the existence of liquid puddle along the valve periphery in Fig. 5(d) ("bright line" along the valve periphery which is due to the reflection of the illuminating light by the puddle). The fuel film under the footprint of fuel spray quickly runs down the port wall and the surface of the valve back by gravity, and gathering along the valve periphery. Since the intake valve is closed, the effect of shear force on the fuel film due to the intake mixture motion is negligible. The phenomenon observed in Fig. 5, however, was clear only right after engine starting (significant film accumulation is completed by then) and during the early stage of warm-up. Beyond the period, the film accumulation along the valve periphery waned away as coolant temperature increased. The main reason is related with the behavior of film thickness. Its effect could be estimated as

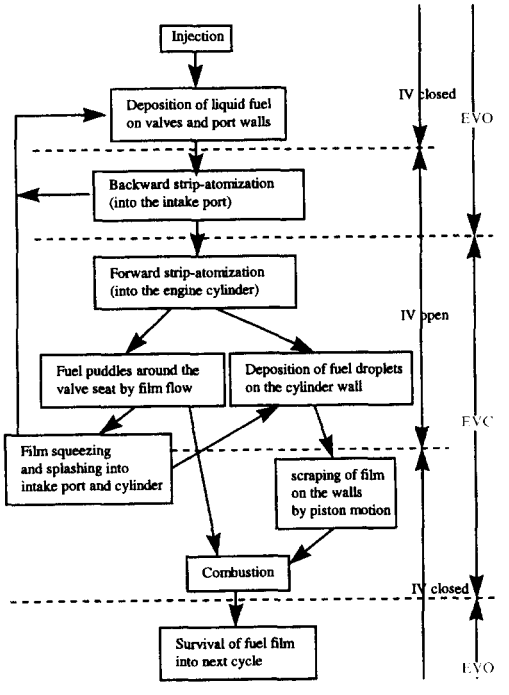

Fig. 4 Sequence of liquid fuel behavior over one cycle during engine warm-up

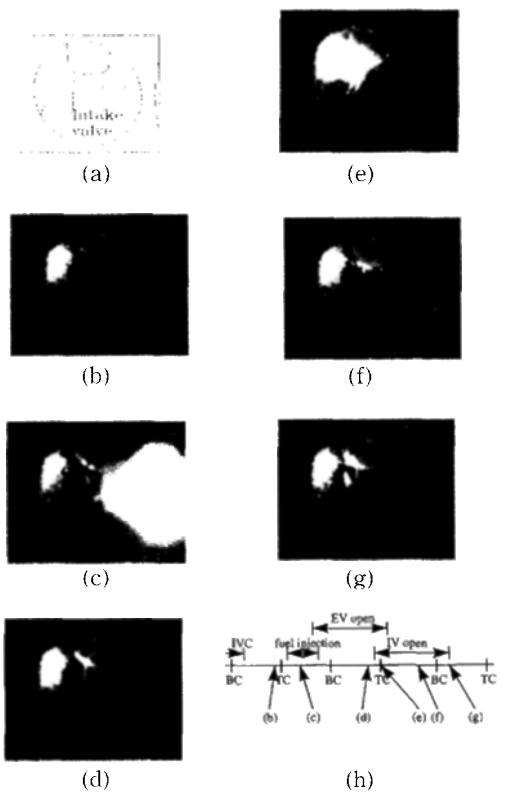

Fig. 5 Liquid fuel behavior in the intake port over one cycle: (a) reference sketch, (b) after IVC and before fuel injection, (c) fuel injection, (d) after fuel injection and before IVO, (e) backward strip-atomization by the overlap back-flow, (f) forward flow, (g) shaking of liquid fuel off the valve stem during valve closing, and (h) time line of an intake event

follows. Assuming that the inertial terms in the Navier-Stokes equation are negligible, the force balance between the gravity and viscous terms can be approximated as follows :

$$\rho g \sim \mu u / \delta^2 \tag{1}$$

From the above relation, the mean film velocity $u \sim \rho g\ \delta^2/\mu$ where δ is the film thickness. During engine starting and the early stage of warm-up when film accumulation in the intake port is significant due to unfavorable fuel evaporation environment, most of the liquid film flows down the back of the intake valve and the port walls, being accumulated along the periphery of the intake valve. It is worthwhile to estimate the film thickness which causes the observed film flows by gravity. According to a simulation model about film flows (Iwano et al., 1991), the fuel film thickness is about 100 μm at 80 ℃ of coolant temperature and 200 μm at 40 ℃. Therefore, the film thickness right after starting and during the early stage of warm-up, would be larger than at least 200 μm. When the film thickness is assumed to be of the order of 500 μm under the footprint of fuel spray, the film velocity becomes ~0.25 m/sec. Under the engine speed of 1200 rpm, the film moves more than 2 cm during the intake valve closing period (600 CA). The film velocity is fast enough for the fuel films near the valve to gather along the periphery of the valve. When the film thickness becomes less than 200 μm, the film velocity becomes so small that the gravity effect may be neglected. It is also consistent with the port visualization result.

And as soon as the intake valves start to open, the in-cylinder gas blows back into the intake port because the in-cylinder pressure is still higher than the intake manifold pressure. The blow back occurs during the valve overlap period during which the intake and exhaust valves are open and hence the in-cylinder pressure is about the same as the exhaust pressure. Since the initial blow back is very strong, it strips off the film accumulated along the periphery of the intake valves in form of atomized droplets. The backward strip-atomization results in the redistribution of the liquid fuel over the intake port. The liquid fuel behavior in the intake port over one cycle is observed in the sequence of the pictures in Fig. 5.

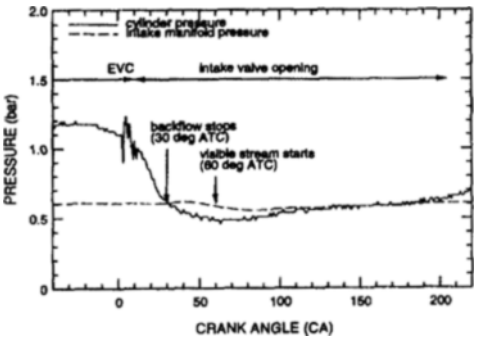

Fig. 6 Cylinder and intake manifold pressures during intake process

The forward mixture induction immediately follows the backward strip-atomization. The event can be observed within the cylinder from the in-cylinder visualization results. Figure 6 shows the pressure traces in the intake port and engine cylinder synchronized with the sequence of video frames in Fig. 7 showing the entry of the droplet mist into the cylinder. When the intake valve opens, no fuel droplet stream could be observed initially. This is because the cylinder pressure then is higher than the pressure in the intake manifold (see Fig. 6), and there is a back flow of the charge into the intake port (Cheng et al, 1991) as observed in Fig. 5. The back flow stops when the cylinder pressure equilibrates with that of the intake manifold; then visible droplet stream begins to enter the cylinder as the intake forward flow commences. (There is a delay between the time of pressure equilibration which is at 30 ℃ after TC in Fig. 6, and the first appearance of the fuel drops at 60 ℃ after TC. The delay will be discussed in the next section.) The entry of the droplet mist is observed as a fuzzy obscuration of the image. Flow of liquid into the cylinder is also observed. The liquid manifests as substantial puddles with wavy surfaces residing around the intake valve seat and on the valve face. Note also that around the periphery of the valve, there is a substantial liquid film that survives combustion in the previous cycle.

When the intake valve closes, the puddles at the

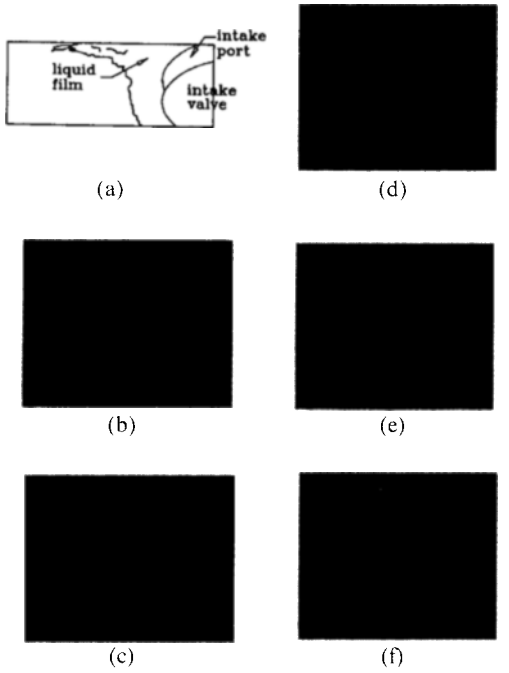

Fig. 7 Sequence of pictures showing visible droplet stream in the intake process right after start-up: (a) Reference sketch, (b) 57° ATC (intake stroke), (c) 60°ATC (intake stroke), (d) 63°ATC (intake stroke), (e) 66°ATC (intake stroke), and (f) 69°ATC (intake stroke)

valve seat are squeezed between the valve lip and valve seat. The squeezed film is broken up into fairly large droplets (estimated to be ~1 mm diameter from the video) which splashes into the cylinder. When these large drops land on the head and liner walls, they form significant isolated puddles. These wall puddles stay in place due to surface tension.

5. Important Features of Liquid Fuel Behavior

To clarify the features of liquid fuel behavior within the cylinder, the following topics will be described in detail:

1) backward strip-atomization of liquid fuel by the blow-back gas

2) forward strip-atomization of liquid fuel by the intake flow

3) fuel film accumulation on the valve surface and seat area

4) liquid film squeezing by the closing valve

5) the in-cylinder liquid film distribution

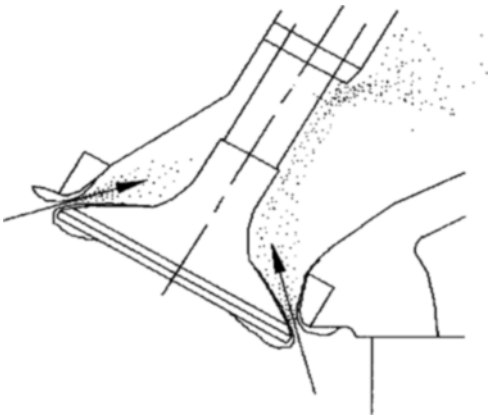

Fig. 8 Backward strip-atomization of liquid fuel by the blow-back gas

5.1 Backward strip-atomization of liquid fuel by the blow-back gas

When the intake valve opened, the intake port pressure (0.5 bar) was lower than the cylinder pressure (~ atmospheric) and there was a strong blow-down (almost sonic) from the cylinder to the intake port. This flow was further sustained by the valve overlap (16° overlap, see Table 2) so that there was flow from the exhaust port to the cylinder. The strong back flow stripped off and shear-atomized the liquid film at the port wall and at the back of the intake valve into droplets. Figure 8 illustrates the process. These droplets were carried by the back flow up the intake port and appeared as a strong glare in Fig. 5(e). The large droplets deposited on the port walls and valve stem. The small droplets might suspend in the air and, later, be transported into the cylinder during the forward flow.

5.2 Forward strip-atomization of liquid fuel by the intak flow

The observed dominant atomization process for the liquid fuel is the stripping off droplets from the fuel film on the port, intake valve stem, and back-of-intake-valve surfaces by the shear stress of the intake flow. Because in the intake-geometry

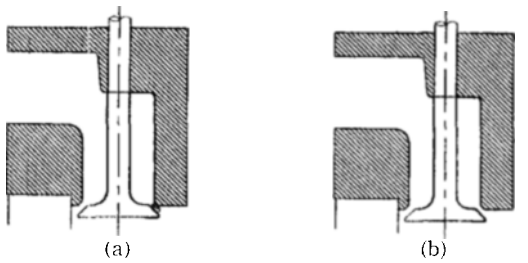

Fig. 9 Forward strip-atomization by (a) high intake air velocity, (b) low intake air velocity.

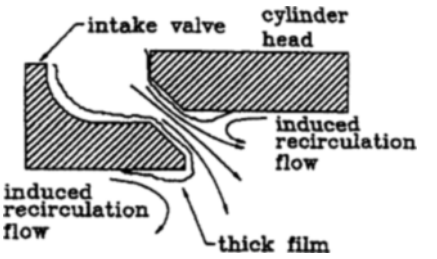

Fig. 10 Formation of thick liquid film at the vicinity of the valve lip and seat

used, most of the fuel spray from the injector landed on the port surface, the above process was dominant both for closed-valve and open-valve injections. The process is illustrated in Fig. 9. When the air flow velocity is high (when the valve is not fully lifted and when the piston is at ~mid-stroke), a fine and dense mist of droplets is formed (Fig. 9(a)). Since the droplet size is inversely proportional to the Weber number of the flow ($We=\rho V^2/(\sigma/\delta)$), the fine mist wanes into a stream of large and sparsely distributed droplets at the later part of the intake process when the intake air velocity is small, i. e. when the valve is fully lifted and the piston is close to the end stroke (Fig. 9(b)).

The delay (see Fig. 6) between the stop of the back flow and the observed start of the droplet stream may be attributed to the fact that effective atomization does not start until there is sufficiently high intake air velocity, which is dependent on the valve lift and the piston velocity. (Except for the first few cycles, the delay is not due to the fuel film transport at the port because a liquid film from the previous cycles is always present).

5.3 Fuel film accumulation on the value surface and seat area

The fuel deposited in the valve stem, back of the intake valve and the port surfaces is pushed towards the cylinder as a film-flow by the shear stress of the intake flow and gravity. This film flow stops, however, at the valve exit because of the diverging flow field as the intake air enters the cylinder (see Fig. 10). The recirculation region induced by the air flow at the valve face and at the head area next to the valve seat traps the film at the lip of the valve face and at the valve seat and its vicinity. The film thickness of the film would be determined by a balance between the surface tension, the shear force produced by the air flow and gravity. The accumulation of liquid film is especially significant towards the end of the intake process because of the reduced amount of shear-atomization, and because in most practical cases, the intake valve closes at part way into the compression stroke so that there is a reverse displacement flow then.

When the wall temperature is cold, a good fraction of the liquid in many of the in-cylinder fuel films, especially those on the valve surface and around the valve seat on the head, survive combustion into the next cycle in the early cycles of the warm-up process.

5.4 Liquid film squeezed by the closing valve

As discussed in the above, there is substantial accumulation of liquid films on the valve lip and the valve seat at the end of the intake process. When the valve closes, these fuel films are squeezed by the impact of the lip on the seat. The liquid is squeezed into large droplets which splash into the cylinder and intake port (see Fig. 11). The splashing of the fuel drops are clearly visible. The drop size estimated from the images is of the order of 1 mm. These big drops land on the head and the cylinder wall to form the substantial puddles.

5.5 In-cylinder liquid film distribution

Based on the flow visualization results, the liquid film distribution may be divided into three

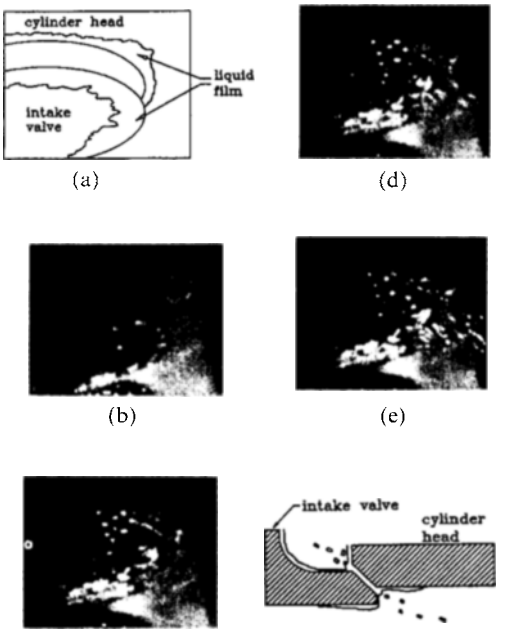

Fig. 11 Film squeezing phenomenon: (a) reference sketch (b) 40°BBC (compression) (c) 25° ABC (compression) right after film squeezing (d) 30.4°ABC (compression) (e) 41.2°ABC (compression) (f) sketch showing film squeezing mechanism

types, according to the process by which they are formed (see Fig. 12).

(1) A thick film at the valve surface and around the valve seat - This film is formed by the liquid film flow from the back of the valve and the port surfaces.

(2) A thin film on the combustion chamber surfaces formed by the impingement of the droplet stream from the strip-atomization.

(3) Isolated puddles formed by the landing of the splashed drops from the intake valve closing process.

The latter two types of liquid film disappear quickly in the combustion process even at the very early stage of the warm-up process. The thick film around the valve area, however, survives combustion into the next cycle well into the warm -up period (of the order of 1 minute after firing).

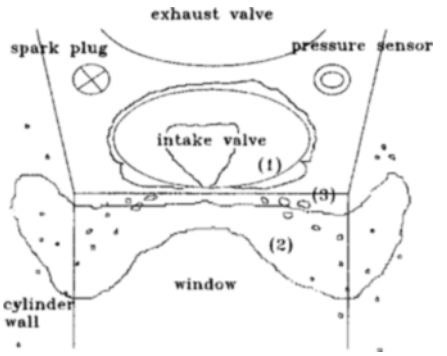

(1) Film around intake valve
(2) Film from droplet stream
(3) Film from splashing droplets

Fig. 12 Typical in-cylinder film distribution

6. Engine Warm-Up Behavior

The engine warm-up behavior is discussed in this section. The warm-up experiments were done using indolene as fuel at the speed fixed at 1,000 rpm and at the intake pressure of ~0.5 bar. The fuel was injected at stoichiometry with closed-valve injection timing. The liquid fuel behavior was compared for the two different type of injector configuration.

6.1 Visualized liquid feul behavior

The comparison is shown in Fig. 13. The significant in-cylinder liquid films are those around the intake valve. The sketches in Fig. 13 were based on the video images at 30, 60 and 90 seconds since injection started. Compared to the normal injector results, there is substantially more liquid in the cylinder and the liquid film persists longer with the air-assisted injector. This difference, again, may be attributed to the injection geometry. In the case of the normal injector (Fig. 3(a)), the foot print of the fuel spray in the port has a large area which facilitates vaporization in the port. (The facilitation is due to two (related) factors. When the fuel is spread over a larger area, the energy required per unit area to evaporate the fuel is less. The surfaces are less cooled by the fuel so that the temperature is higher which facilitates heat transfer and the evaporation of the heavier

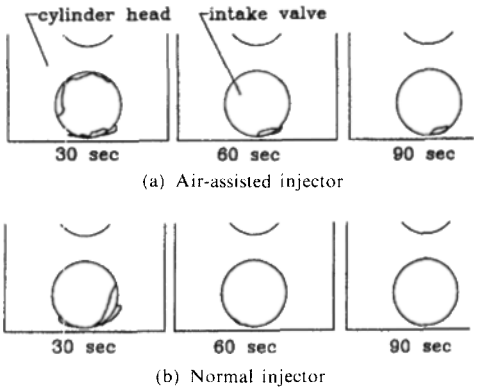

Fig. 13 Fuel film behavior with respect to fuel injector configuration during warm-up (A/F =14.6, closed-valve injection)

fuel components.) As a result, the film flow is reduced. For the air-assisted injector, because of the proximity of the injector tip to the back of the valve (Fig. 3(b)), most of the fuel land on a small area, and there is a substantial film flow into the cylinder.

6.2 Temperature behavior of the intake system

Because the fuel evaporation process is highly temperature dependent, the temperatures of selected components of the intake system were measured in the warm-up process. These measurements will also elucidate the differences between the fuel injection configurations.

The apparatus is shown in Fig. 14. The measurement consisted of the port surface temperature at 43.0 mm from the cylinder entrance, and the temperatures at the back of the intake valve which was pinned so that the valve orientation was fixed. For the latter, two measurement locations were used. They were opposite each other along a diameter which was parallel to the line connecting the centers of the intake and exhaust valves. The two measurements will be referred to as the temperature of the intake valve at the intake side (denoted by A) and at the exhaust side (denoted by B).

The major factor affecting the temperature of the intake system is the back flow of the burned gas from the cylinder to the intake when the valve

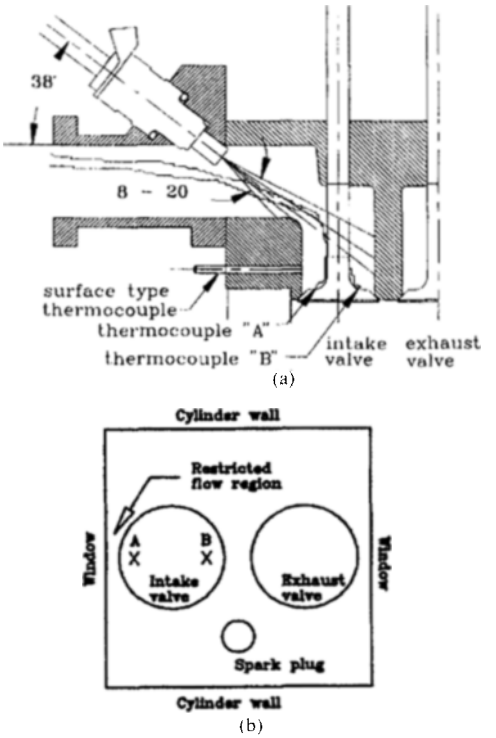

Fig. 14 Temperature measurements in the intake system; (a) section side view (b) top view

opens. To study this phenomenon, the engine was operated first with propane fuel (which was injected into the intake port) so that complication due to the cooling of the valve by the impingement of the liquid was absent. The temperature measurement results for closed valve injection are shown in the first portion (at time t less than 60 seconds, with start of fueling at time zero) of Fig. 15. The temperatures at the back of the intake valve are higher than that of the port wall which has much higher thermal inertia.

The difference in temperature between the two locations on the intake valve was the result of different heat transfer from the valve seat. In valve heat transfer mechanism, most of heat is lost through the valve contact because of the wide contact area and the high heat transfer coefficient associated with metal-to-metal contact. The valve seat area close to the thermocouple position B is hotter than that to the position A, because the position B is closer to the hot exhaust valve and valve seat. Therefore, the uneven temperature

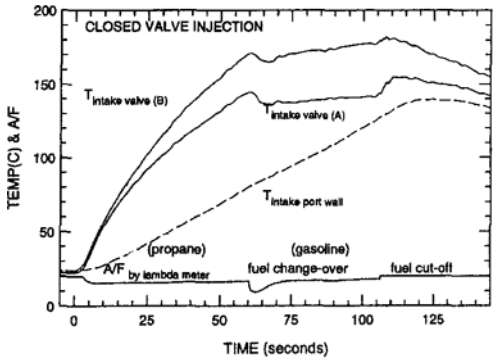

Fig. 15 Intake system component temperatures during warm-up (p_i=0.5bar, λ=1.0, 1,000 rpm). Liquid fuel was delivered by the normal injector in closed-valve injection

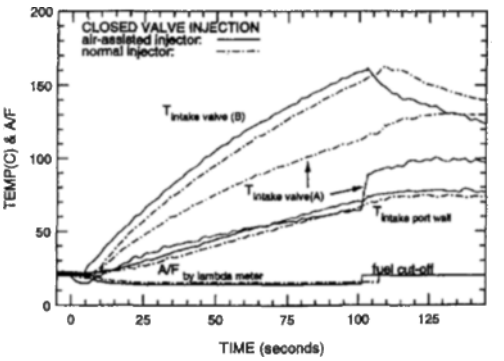

Fig. 16 Intake system component temperatures during warm-up for different injector configurations. (A/F=14.6, closed-valve injection)

distribution along the valve seat resulted in the temperature difference between the positions A and B.

The propane injection was switched off at t=60sec in Fig. 15, and gasoline injection using the normal injector with closed-valve injection was switched on for t=60 to 120 sec. The "step" drop of temperatures at the back of the intake valve was due to the liquid fuel cooling effect (Martins and Finlay, 1992). There was no step-decrease in the port wall temperature because the measurement location was in a shadow outside the footprint of the fuel spray.

The intake system component temperatures during warm-up using the air-assisted injector and the normal injector with the closed-valve injection are compared in Fig. 16. For both configurations, the temperatures in location A were lower than those in location B due to the back flow pattern as described above. For the air-assisted injector, however, there was the extra factor due to the significant fuel spray impingement at location A; thus a considerably lower temperature was measured at location A.

One important thing to note is that the forward strip-atomization persists during the whole period regardless of the injector configuration. The disappearance of liquid fuel on the valve face at 90 seconds for the normal injection necessarily means complete fuel evaporation. Although the strip-atomized mist that couldn't be shown in the printed pictures, it was visible in the video segment. The mist seems to be formed by the strip-atomizing of the fuel film on the port wall around the valve seat where the temperature is still low compared to the valve temperature as shown in Fig. 16. Therefore, as far as the port wall temperature is low, the entry of liquid fuel into the cylinder is inevitable. The mist lands on the wall and a fraction of the mist will survive combustion process because it stays within the flame quenching layer. Its evaporation during the exhaust process contributes to high level of hydrocarbon emissions which is typical during warm-up.

7. Conclusions

The liquid fuel behavior in the intake port and the cylinder during starting and warm-up was visualized through visualization windows using a high speed CCD camera. There is significant liquid fuel entry into the cylinder, in particular, during the early cycles in the warm-up process. The major liquid fuel transport processes are: the backward strip-atomization of the fuel film along the periphery of the intake valves by the valve overlap backflow, the forward strip-atomization of the fuel film on the surfaces of the intake system into droplet streams by the intake air flow; the film flow which forms significant liquid puddles at the valve surface and at the vicinity of the intake valve; and the squeezing of the liquid film at the valve lip and seat into large droplets in the

valve closing process. A substantial fraction of the liquid in the thick film formed at the valve surface and the seat area survives combustion into the next cycle. The time evolution of the in-cylinder liquid film is influenced by the injection geometry.

References

Cheng, C. O., Cheng, W. K., Heywood, J. B., Maroteaux, D. and Collings, N., 1991, "Intake Port Phenomena in a SI Engine at Part Load," *SAE Paper* 912401.

Cheng, W. K., Hamrin, D., Heywood, J. B., Hochgreb, S., Min, K-D., and Norris, M., 1993, "An Overview of Hydrocarbon Emissions Mechanisms in Spark-Ignition Engines," *SAE Paper* 932078.

Fox, J. W., Min, K-D., Cheng, W. K. and Heywood, J. B., 1992, "Mixture Preparation in a SI Engine with Port Fuel Injection During Starting and Warm-up," *SAE Paper* 922170.

Iwano, H., Jaitoh, M., Sawamoto, K. and Nagaishi, H., 1991, "An Analysis of Induction Port Fuel Behavior," *SAE paper* 912348.

Martins, J. J. G. and Finlay, I. C., 1992, "Fuel Preparation in Port Injected Engines," *SAE Paper* 920518.

Meyer, R., 1997, "In-Cylinder Liquid Fuel Droplet Measurements," *Massachusetts Institute of Technology, Engine and Fuel Research Consortium*, Feb. 20.

Namazian, M., Hansen, S. P., Lyford-Pike, E. J., Sanchez-Barsse, J., Heywood, J. B. and Rife, J., 1980, "Schlieren Visualization of the Flow and Density Fields in the Cylinder of a Spark-Ignition Engine," *SAE Paper* 800044.

Yang, J., Kaiser, E. W., Siegl, W. O. and Anderson, R. W., 1993, "Effects of Port-Injection Timing and Fuel Droplet Size on Total and Speciated Exhaust Hydrocarbon Emissions," *SAE Paper* 930711.